THE JOURNAL OF PHYSICAL CHEMISTRY B

ARTICLE

pubs.acs.org/JPCB

Reaction Kinetics of Catalyzed Competitive Heteropolymer Cleavage

S. Kashif Sadiq,*,† Balázs Könnyü,‡ Viktor Müller,‡ and Peter V. Coveney§

†Computational Biochemistry and Biophysics Laboratory (GRIB-IMIM), Universitat Pompeu Fabra, Barcelona Biomedical Research Park (PRBB), C/Doctor Aiguader 88, 08003 Barcelona, Spain

‡Institute of Biology, Eötvös Loránd University, Pázmány P. s. 1/C, 1117 Budapest, Hungary

§Centre for Computational Science, Christopher Ingold Laboratories, University College London, 20 Gordon Street, WC1H 0AJ, London, United Kingdom

ABSTRACT: A theoretical formulation for complete heteropolymer degradation is developed in terms of Michaelis−Menten reaction kinetics under the quasi-steady-state approximation. This allows the concentration of the entire intermediate decomposition cascade to be accounted for as well as each species of emerging final product. The formulation is implemented computationally and results in stable reaction kinetics across a range of orders of magnitude for K_M and k_{cat}. The model is compared with experiment, specifically in vitro HIV-1 protease-catalyzed retroviral Gag-polyprotein processing. Using an experimentally determined cleavage-polypeptide parameter set, good qualitative agreement is reached with Gag degradation kinetics, given the difference in experimental conditions. A parameter search within 1 order of magnitude of variation of the experimental set results in the determination of an optimal parameter set in complete agreement with experiment which allows the time evolution of each individual as well as intermediate species in Gag to be accurately followed. Future investigations that determine the required enzymatic parameters to populate such a scheme will allow for the model to be refined in order to track the time for viral maturation and infectivity.

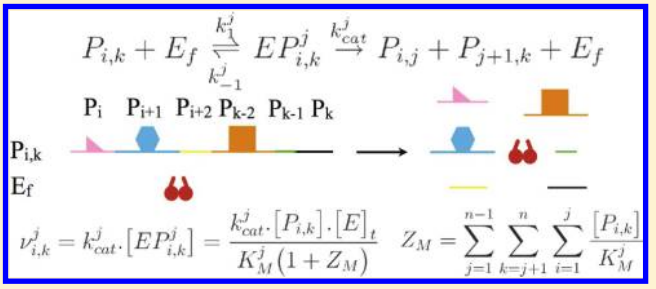

I. INTRODUCTION

Predictive mechanistic modeling of complex molecular interactions that results in the accurate description of emergent higher-scale biochemical function remains one of the outstanding challenges in theoretical chemistry. From pioneering theoretical investigations in embryo development[1] into what has in more recent decades emerged as systems biology,[2] mechanistic modeling techniques have most commonly used chemical reaction kinetics schemes that employ the law of mass action to describe the interactions of an array of processes that result in regulation and modulation of the overall system.[3] In particular, the investigation of many aspects of complex biological systems including cell signaling pathways,[4] metabolism,[5] cell-cycle regulation,[6] and origin of life studies[7] have been undertaken previously. A key feature of enzyme-mediated reaction networks has been the widespread applicability of the Michaelis−Menten (MM) equation:[8]

$$\nu = k_{cat}\cdot[ES] = \frac{k_{cat}\cdot[S]\cdot[E_t]}{K_M + [S]} \quad (1)$$

where ν denotes the rate of enzymatic processing of a single species of substrate with one cleavage site, [S] denotes the substrate concentration, $[E_t]$ the total enzymatic concentration, [ES] the concentration of the enzyme−substrate complex, k_{cat} the catalytic turnover rate constant, and K_M the Michaelis−Menten constant, derived under the steady-state approximation[9] in which the rate of change of the concentration of enzyme-bound substrate is assumed to be zero ($d[ES]/dt = 0$).

For the case of competitive multiple species substrate cleavage in which $n - 1$ distinct single-cleavage site substrate species (S_1, S_2, ..., S_{n-1}) compete for the same enzyme active site, the MM equation describing the processing of each species can be attained by making the quasi-steady-state approximation (QSSA)[10] for each species

$$\nu^r = k^r_{cat}\cdot[ES^r] = \frac{k^r_{cat}\cdot[S_r]\cdot[E_t]}{K^r_M(1 + \sum_{j=1}^{n-1}[S_j]/K^j_M)} \quad (2)$$

where ν^r and $[S_r]$ refer to the reaction rate and concentration of the rth substrate respectively and $[ES^r]$ to the concentration of enzyme bound to S_r. Although not feasible in some situations,[11] the use of the quasi-steady-state approximation[10] to derive the MM rate equations has nonetheless proved robust in many situations over time.

Many biochemical and physicochemical processes involve either the ordered stepwise or competitive catalytic processing of polymers with multiple cleavage sites into their distinct constituents. For example, enzyme-catalyzed heteropolymer cleavage is

Received: July 5, 2011
Revised: August 4, 2011
Published: August 08, 2011

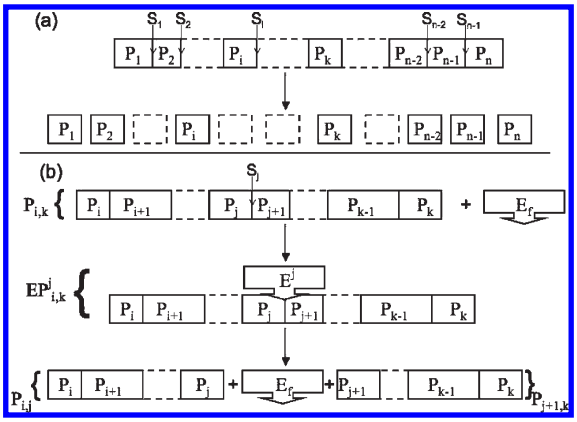

Figure 1. (a) Schematic representation of the decomposition of an n-chain heteropolymer ($P_{1,\,n}$) into n distinct units. Cleavage sites are labeled $S_1 \ldots S_{n-1}$. (b) Schematic representation of the binding and subsequent cleavage of an intermediate heteropolymer by a free catalyst molecule. The catalyst molecule E_f binds to an intermediate polymeric chain, $P_{i,\,k}$, consisting of all monomers between and including monomer P_i and P_k, at the binding site between two adjacent monomers P_j and P_{j+1}, thus forming a polymer−catalyst complex, $EP^j_{i,\,k}$. Cleavage of the intermediate heteropolymer at the S_j site results in the formation of two further intermediate polymers, $P_{i,\,j}$ and $P_{j+1,\,k}$, as well as liberation of the free catalyst molecule E_f.

a ubiquitous phenomenon in the chemistry of polypeptide, polynucleotide, and polysaccharide degradation and recycling.[12] Theoretical formalisms based on the MM equation for such classes of catalyzed polymer degradation are well established. These include descriptions of both homo- and heteropolymer systems[13] which undergo either repeated stepwise[14,15] or competitive cleavage. Furthermore, the description of stepwise cleavage has been extended to include mixed polymer systems.[16]

Hanson[13] has shown that eq 2 equivalently describes the competitive decomposition of a heteropolymer species in terms of the concentration of each cleavage site. For experimental techniques in which enzymatic activity is monitored through the net increase of cleavage, this is sufficient.[17] However, the major drawback of such a formulation is that it does not account for the concentrations of individual distinct species (monomer or intermediate) in the decomposition cascade. For the range of biochemically relevant applications in which such accounting is necessary, a new formulation is thus needed, and, despite the complexity of previous models constructed, the full degradation cascade of a heteropolymer has remained undeveloped.

A specific example arises in the enzyme-catalyzed cleavage cascade of polyproteins into individual protein units. All retroviral and specifically HIV maturation is critically dependent on the rate at which structural capsid (CA) proteins are liberated from Gag and Gag-Pol polyprotein precursors encoded by the viral genome and processed by the viral protease.[18] Experimental investigation of the in vitro time course of the cleavage cascade is now routine[19] as well as perturbation with respect to rate enhancing/decreasing mutation.[20]

Here, we develop a Michaelis−Menten style scheme specifically deriving expressions to account for the concentrations of each species in the entire decomposition cascade of a heteropolymer of arbitrary length, not just the concentrations of cleaved substrate. Furthermore, we detail the general kinetic properties of the scheme as well as its sensitivity to parameter variation. We investigate the applicability of such a formulation in describing in vitro HIV-1 protease-catalyzed Gag polyprotein cleavage by comparing a numerical implementation of the formulation to existing experimental data.[19] The ability to completely quantitatively compare such models with experiment requires the existence of kinetic parameters measured in the same conditions as the overall phenomena under investigation. In line with the prevalent problem in complex reaction network modeling,[21] such parameter completeness is not available. However, despite the sparseness of available data, a qualitative comparison is made using the nearest complete data set. Furthermore, in order to test whether an appropriate parameter set would give the correct kinetics, a parameter search is conducted within 1 order of magnitude variation for each cleavage site of Gag, resulting in a complete correlation with experiment.

II. THEORETICAL DEVELOPMENT

Consider an n-chain heteropolymer (denoted $P_{1,\,n}$) undergoing catalytic decomposition into n units (see Figure 1a). The individual monomers are labeled sequentially P_1, P_2, ..., P_n. Catalytic cleavage occurs through a decomposition cascade of $P_{1,\,n}$ through a range of intermediate polymers into the final set of cleaved monomeric units. In eq 2, for any given substrate species, there is an equivalence between the loss in cleavage site concentration and gain in corresponding product concentration because singular-cleavage results in final processing of that substrate. For a heteropolymer, this is no longer the case because all substrate species are linearly connected and emerging products from one reaction serve as substrate in another until all intermediate species have been processed. In order to formulate a reaction kinetics scheme that takes into account the time evolution of the final species, it is thus necessary to view the system in terms of the concentrations of each possible species.

Let $P_{i,\,k}$ represent an intermediate heteropolymer composed of all monomers between and including the ith and kth monomeric units while P_j and P_{j+1} denote two neighboring monomers within $P_{i,\,k}$ between which a free catalyst molecule (denoted by E_f) binds and cleaves (see Figure 1b). The reaction results first in the formation of a bound catalyst−polymer substrate complex, denoted $EP^j_{i,k}$, followed by cleavage into two further intermediate chains, $P_{i,\,j}$ and $P_{j+1,\,k}$, as well as liberation of the original catalyst molecule E_f.

The kinetic scheme for the reaction is given by eq 3

$$P_{i,\,k} + E_f \underset{k^j_{-1}}{\overset{k^j_1}{\rightleftharpoons}} EP^j_{i,\,k} \xrightarrow{k^j_{cat}} P_{i,\,j} + P_{j+1,\,k} + E_f \qquad (3)$$

where k^j_1 and k^j_{-1} are the forward and reverse rate constants for the formation of the $EP^j_{i,\,k}$ complex respectively, while k^j_{cat} is the rate constant for the subsequent catalytic cleavage of $EP^j_{i,\,k}$ into products. Here, we make the assumption that association, dissociation, and catalytic rate coefficients are dependent only on the specificity of the cleavage site and not on the specificity and number of adjacently bound monomeric units either side of the cleavage region. The total concentration of catalyst, $[E_t]$, is conserved such that

$$[E_t] = [E_f] + [E_b] \qquad (4)$$

where $[E_f]$ and $[E_b]$ are the concentrations of free and bound catalyst respectively. In general, at any one time, there is a nonzero concentration of all intermediate polymer−catalyst complexes. Using the i, j, k summation convention for the

intermediate complex element, $EP^{j}_{i,k}$, the latter term in eq 4 can thus be expressed by summing over all possible intermediate combinations of $EP^{j}_{i,k}$ from an n-chain heteropolymer such that

$$[E_b] = \sum_{j=1}^{n-1} \sum_{k=j+1}^{n} \sum_{i=1}^{j} [EP^{j}_{i,k}] \tag{5}$$

Under the quasi-steady-state approximation, the rate of change of the intermediate complex $d[EP^{j}_{i,k}]/dt = 0$. It thus follows that for a given complex, $EP^{j}_{i,k}$, the rate of change can be expressed as

$$k^{j}_{1}[P_{i,k}]\cdot[E]_f - k^{j}_{-1}[EP^{j}_{i,k}] - k^{j}_{cat}[EP^{j}_{i,k}] = 0 \tag{6}$$

where the first term on the LHS represents the forward rate of production of $EP^{j}_{i,k}$ from the association of heteropolymeric chain $P_{i,k}$ and the catalyst E_f, the second term represents the reverse dissociation rate, and the third term represents the rate of decomposition into product. Rearranging eq 6 and using the Michaelis−Menten relation for the process ($K^{j}_{M} = (k^{j}_{-1} + k^{j}_{cat})/(k^{j}_{1})$), we obtain the concentration of a given intermediate complex, $EP^{j}_{i,k}$, in terms of the concentration of the precursor $P_{i,k}$ and the free catalyst concentration $[E_f]$

$$[EP^{j}_{i,k}] = \frac{1}{K^{j}_{M}}[P_{i,k}]\cdot[E_f] \tag{7}$$

It thus follows from eq 5 that the total concentration of bound catalyst $[E_b]$ is

$$[E_b] = Z_M\cdot[E_f] \tag{8}$$

where

$$Z_M = \sum_{j=1}^{n-1} \sum_{k=j+1}^{n} \sum_{i=1}^{j} \frac{[P_{i,k}]}{K^{j}_{M}} \tag{9}$$

Equation 8 is important as it states that, under quasi-steady-state conditions, the concentration of bound catalyst is proportional to the concentration of free catalyst by a factor, Z_M, the summed ratio over all possible intermediate precursors and corresponding Michaelis−Menten parameters for each cleavage point. This allows the concentration of the intermediate complex to be determined as a function of the total catalyst concentration $[E_t]$, which remains constant. By substituting eq 4 into eq 7, making use of eqs 8 and 9 and rearranging we obtain

$$\nu^{j}_{i,k} = k^{j}_{cat}\cdot[EP^{j}_{i,k}] = \frac{k^{j}_{cat}\cdot[P_{i,k}]\cdot[E]_t}{K^{j}_{M}(1 + Z_M)} \tag{10}$$

where $\nu^{j}_{i,k}$ is the rate of cleavage of the intermediate complex $EP^{j}_{i,k}$.

This formulation is consistent with that of eq 2 which stems from the perspective of accounting for cleavage site concentrations rather than individual species. The concentration of a given cleavage site is equal to the concentration of all possible polymer species that contain it:

$$[S_j] = \sum_{i=1}^{j} \sum_{k=j+1}^{n} [P_{i,k}] \tag{11}$$

However, the rate of change of concentration of a given cleavage site is only dependent on the forward reaction into products of a polymer species that contains that site. The rate is then the sum of the forward rates of cleavage at that site for all possible polymer species that contain the site. We therefore have

$$\nu^{j} = \sum_{i=1}^{j} \sum_{k=j+1}^{n} \nu^{j}_{i,k} = \frac{k^{j}_{cat}\cdot \sum_{i=1}^{j} \sum_{i=1}^{j} [P_{i,k}]\cdot[E]_t}{K^{j}_{M}(1 + Z_M)} \tag{12}$$

and by substituting eq 9 and 11 into eqs 12 we recapture the conventional Michaelis−Menten formulation of eq 2.

The absolute rate of production, $\nu_{i,k}$, of any intermediate species, $P_{i,k}$, can be expressed by accounting for three things: (a) production of $P_{i,k}$ from any intermediate polymer with a longer head terminal but which terminates at P_k ($P_{1,k}...P_{i-1,k}$), (b) production of $P_{i,k}$ from any intermediate polymer with a longer tail terminal but which begins with P_i ($P_{i,k+1}...P_{i,n}$), and finally (c) cleavage of $P_{i,k}$ at any possible cleavage site j. We thus have for $i \neq k$

$$\begin{aligned} \nu_{i,k} &= d[P_{i,k}]/dt \\ &= \sum_{a=1}^{i-1} \nu^{i-1}_{a,k} + \sum_{b=k+1}^{n} \nu^{k}_{i,b} - \sum_{j=i}^{k-1} \nu^{j}_{i,k} \end{aligned} \tag{13}$$

An expression for the overall rate of production (ν_i) of any individual monomer (P_i) can then be obtained by summing over all the rates of production from each possible intermediate complex from which the monomer P_i is immediately derived. For an n-chain heteropolymer, this is given by

$$\nu_i = d[P_i]/dt = \sum_{a=1}^{i-1} \nu^{i-1}_{a,i} + \sum_{b=i+1}^{n} \nu^{i}_{i,b} \tag{14}$$

Equations 13−14 allow us to account for the change in concentration of each intermediate and final species in the decomposition cascade. They describe a set of coupled ordinary differential equations, where the concentration of any polymer species is dependent on every other polymer species in the decomposition cascade. Given an initial concentration of heteropolymer, a catalyst concentration, and a K_M and k_{cat} parameter set for all the cleavage sites, these equations can be integrated numerically in order to determine the concentration of each species over time.

III. RESULTS

Equations 13−14 were numerically integrated on a computer, and the kinetics for a range of conditions was investigated. Specifically, these were (a) the limiting case of equivalent catalytic parameters at each cleavage site and (b) the effects of catalytic variation by several orders of magnitude for both K_M and k_{cat} at various cleavage sites along a heteropolymer. It is instructive to use a pentamer for the above analysis as it is the smallest polymer which contains end monomers, a central monomer, and non-central embedded monomers. However, we also explicitly analyzed the corresponding relative properties of terminal and embedded polymer evolution for longer polymers. Finally, the formulation developed here was used to investigate the reaction kinetics of Gag polyprotein processing by HIV-1 protease and compared with experiment.

A. Reaction Kinetics of Equivalent Processing. The behavior of the reaction kinetics model in the regime of equivalent parameters for each of the cleavage sites was investigated, for an initial polymer concentration of $[P_{1,5}] = 100$ mM, $[E]_t = 1$ mM,

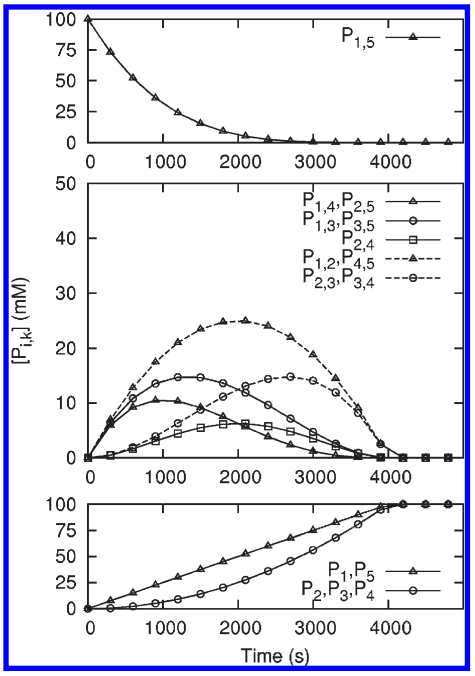

Figure 2. Processing of a heteropentamer $P_{1,5}$ with initial concentration of 100 mM by 1 mM of catalyst for the case of equivalent kinetic parameters at each cleavage site (k_{cat} = 0.1 s^{-1} and K_M = 0.1 mM). The liberation rate of endwise and embedded species are respectively equal (endwise, $P_1 = P_5$, $P_{12} = P_{45}$, $P_{13} = P_{35}$, $P_{14} = P_{25}$ and embedded, $P_2 = P_3 = P_4$, $P_{23} = P_{34}$).

k_{cat} = 0.1 s^{-1}, and K_M = 0.1 mM. Figure 2 shows the time evolution of monomeric and intermediate species. The heteropentamer decays in a well-behaved exponential manner, while the intermediate species arise and fall stably. For any species of a given multimericity, the time evolution varies only depending on whether the multimer is initially embedded within the heteropolymer (requiring two cleavages for liberation) or is an endwise multimer (requiring only one cleavage for liberation). Therefore the liberation rates of endwise monomers are equal to each other ($P_1 = P_5$), as are the evolutions of endwise dimers ($P_{12} = P_{45}$), trimers ($P_{13} = P_{35}$), and tetramers ($P_{14} = P_{25}$) to each other respectively. Likewise, equality of time evolution is respectively exhibited for all embedded monomers ($P_2 = P_3 = P_4$) and dimers ($P_{23} = P_{34}$), irrespective of their positions along the heteropolymer chain (e.g., $P_3 < P_2 = P_4$ is not exhibited).

However, there are significant differences between corresponding embedded and endwise multimers. In particular, the liberation rate of endwise dimers exceeds that of endwise trimers which in turn is faster than that of endwise tetramers. Liberation of embedded dimers lags behind these species and never becomes dominant over endwise dimers. Likewise, the embedded trimer concentration lags behind that of the endwise trimers as well as embedded dimers.

Terminal monomers emerge at a constant rate, while embedded monomers lag behind the terminal ones and exhibit nonlinear emergence. This is expected as the latter require cleavage at two sites instead of just one and naturally depend on the emerging concentration of precursors that are subsequently cleaved into monomer. The linear emergence rate of the former is explained as a special case of equivalence for kinetic parameters k_{cat} and K_M across all cleavage sites (which induces equivalence in the time evolution of all $[S_r]$) coupled with the excess of uncleaved terminal cleavage sites as compared to K_M (where $[S_1] \gg K_M$). This special scenario allows, for example for P_1, the rate of liberation ν_1 of the terminal monomer to be given as (see Appendix for derivation):

$$\nu_1 \approx \frac{k^1_{cat} \cdot [E_t]}{n-1} = \frac{V^1_{max}}{n-1} = \text{constant} \tag{15}$$

For the parameters used here, namely, n = 5, $[E_t]$ = 1 mM, k^1_{cat} = 0.1 s^{-1}, and K^1_M = 0.1 mM, we have ν_1 = 0.025 mM/s as shown by the data in Figure 2. This results in linearity almost until virtually the end of the reaction where the condition that $[S_1] \gg K^1_M$ no longer holds.

Analsyis of longer polymers is facilitated by first defining a characteristic time scale, τ_c, for the completion of the reaction

$$\tau_c \approx \frac{(n-1)[S_0]}{k_{cat}[E_t]} \tag{16}$$

where $[S_0]$ is the initial concentration of starting heteropolymer and n is the number of monomers in the starting heteropolymer. This takes into account the fact that when k_{cat} and K_M are identical for all cleavage sites, all cleavage sites are indistinguishable and so eq 2 reduces to eq 1, where $[S]$ is the total concentration of uncleaved cleavage sites. Figure 3 shows the time evolution for (a) endwise and (b) embedded multimers (m = multimericity) for pentamers (n = 5), decamers (n = 10), and 20-mers (n = 20) in terms of the fraction of time relative to the characteristic time scale (τ_c) for each heteropolymer. The kinetic parameters for each cleavage site are kept the same as before.

First, as before, any given multimer species exhibits the same time evolution as any other of the same length for endwise and embedded multimers respectively. Second, the time evolution also exhibits an identical profile for like multimers that arise from different heteropolymers, even though in absolute terms the time taken for completion scales linearly with the heteropolymer length n. Extending the analysis to longer polymers thus reveals that any heteropolymer, in the case where all cleavage sites have identical kinetic parameters, exhibits symmetric decay and/or growth properties for the corresponding intermediate and final products in terms of the characteristic time scale at which the complete reaction occurs.

The above results manifest an intrinsic difference in the liberation of terminal and embedded monomers due to the difference in positioning along the chain. A natural liberation order thus emerges as a direct consequence of the structure of the reaction kinetics equations and not only because of variation induced by changes in relative kinetic parameters.

B. Variation of Terminal and Embedded Cleavage Site Processsing. Variation of k_{cat} and K_M at each cleavage site has pronounced and differential effects on the liberation rate of each of the species. Figure 4 shows a matrix of monomer concentration profiles from a decaying pentamer for a range of orders of K_M (left to right: 0.001, 0.01, 0.1, 1, 10 mM) and k_{cat} (top to bottom: 0.001, 0.01, 0.1, 1, 10 s^{-1}) at the first cleavage site, S_1, while keeping the kinetic parameters of all other cleavage sites at k_{cat} = 0.1 s^{-1} and K_M = 0.1 mM. The central profile is thus the same as the monomer profile of Figure 2.

Low K_M with low k_{cat} (Figure 4 top left) results in effective inhibition of all monomer species, consistent with a strong-coupling with the first cleavage site but slow actual cleavage. The cleavage site is thus not only processed slowly but also acts as a competitive inhibitor for the processing of all other sites by arresting

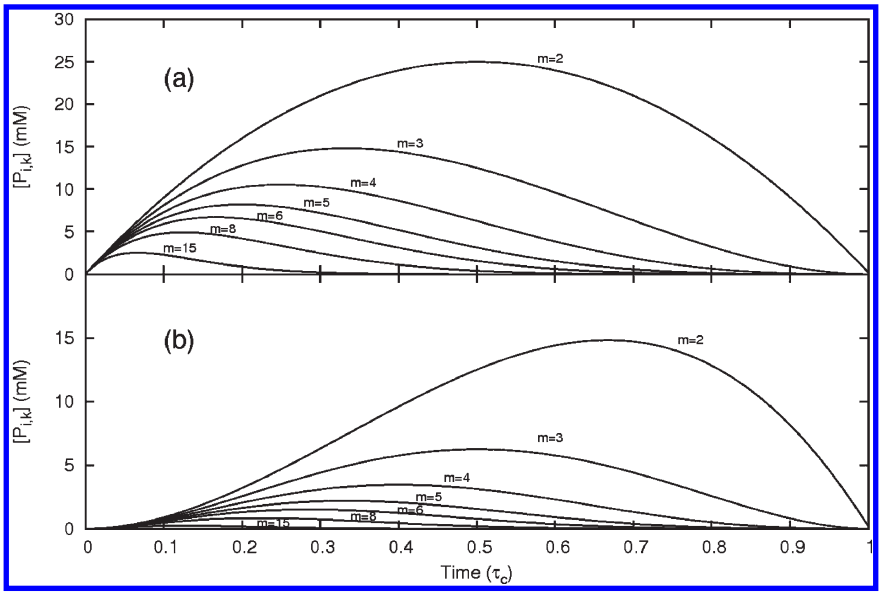

Figure 3. Time evolution of (a) endwise and (b) embedded multimermic (m, multimericity) intermediate species in the decay process of heteropolymers of length n = 5, n = 10, and n = 20 relative to the characteristic time scale (τ_c), defined in eq 16. For a given multimer species, m, the profile of the time evolution in terms of τ_c only depends on whether the species is initially endwise or embedded, not the length of the initial polymer from which it comes. Absolute time evolution scales linearly with heteropolymer length, n (eq 16). For embedded multimers the time evolution is independent of specific location along the heteropolymer. Initial conditions and kinetic parameters are identical to those used in Figure 2.

the enzyme in a practically irreversible form. As K_M increases the cleavage site coupling decreases resulting in reduced inhibition of other cleavage processes, and at high K_M (Figure 4 top right), the kinetics tends to that of a heterotetramer (P_{12}−P_3−P_4−P_5) in which the dimer P_{12} acts effectively as a terminal monomer; the S_1 site is effectively no longer cleaved, nor does it inhibit other cleavage processes.

As k_{cat} increases, the S_1 cleavage site is cleaved faster resulting in an increasing liberation rate of the P_1 monomer (black line) and P_2 monomer (red line). Furthermore, since turnover is increasing, in the low K_M regime (Figure 4 left), this results in reduction of inhibition for other cleavage sites and the increased liberation of the other monomers. At high k_{cat}, low K_M, the first cleavage site is cleaved so fast that the remaining kinetics again tends to that of a heterotetramer (P_2−P_3−P_4−P_5). In the high K_M regime (Figure 4 right), the liberation of other monomers is not affected by the increasing k_{cat}, only the rate of liberation of P_1 and P_2 increases; in the high k_{cat}−high K_M regime the relative reaction kinetics of all monomers is similar to that of the central parameter set albeit slightly faster.

It is in the mid-k_{cat}, mid-K_M regime that the direct effects of altering the terminal cleavage site processing rate are most noticeable. Changing K_M or k_{cat} within 1 order of magnitude either side of equality results in significant changing of the order of liberation of monomer P_1 as compared to the others. Furthermore, as expected, increasing k_{cat} proportionally increases the liberation rate of the P_1 monomer, while increasing the relative K_M induces a lag effect on the processing of the cleavage site and linear processing only commences once the other monomers are mostly liberated.

A similar behavior is exhibited when altering the kinetic parameters of an embedded cleavage site. The only key difference is that as both monomers either side of the cleavage site are themselves embedded, liberation of these monomers is slower than terminal ones when all cleavage sites have equivalent parameters. Thus for any particular value of k_{cat} and K_M at an embedded site, the liberation will be slower than for a terminal site.

This is further examined by comparing the relative integral of the concentration curves (λ) of each monomer species as a function of varying k_{cat} and K_M at each cleavage site (Figure 5), while keeping those of other cleavage sites at 0.1 s^{-1} and 0.1 mM respectively. We define

$$\lambda_i(k^j_{cat}, K^j_M) = \int_0^{\tau_c} \frac{[P_i](k^j_{cat}, K^j_M, t)}{\frac{1}{2}\tau_c[S_0]}dt - 1 \qquad (17)$$

where $\lambda_i(k^j_{cat}, K^j_M)$ corresponds to the integral of monomer P_i while varying the S_j cleavage site, normalized by the integral of a linear liberation process up to the characteristic time scale τ_c and thus varies from 1 (corresponding to an infinitely fast liberation) to −1 (corresponding to no liberation up to τ_c). Given the nonlinearity of the emergence of each species, the above parameter becomes an effective measure of the lead (positive values) or lag (negative values) exhibited by each of the species.

There is a clear difference between the direct and indirect effects of varying kinetic parameters at a given cleavage site, giving rise to four classes of monomer (direct or indirect and terminal or embedded). Direct effects are those on monomers either side of the cleavage site; indirect effects are those on monomers not directly connected. First for cleavage at S_1 (Figure 5a), increase in k_{cat} results in an increase in the liberation rate of both P_1 and P_2, while increase in K_M results in a decrease in liberation rate. The direct effect of parameter alteration is thus compensatory in nature when increasing both parameters; isocontours of liberation rate curve diagonally from low k_{cat}−low K_M to high k_{cat}−high K_M and the same liberation curve can be obtained over a large compensatory variation of both k_{cat} and K_M. P_1 is much more sensitive to parameter variation than P_2 with a more pronounced gradient. At high k_{cat} and low K_M, P_1 is cleaved

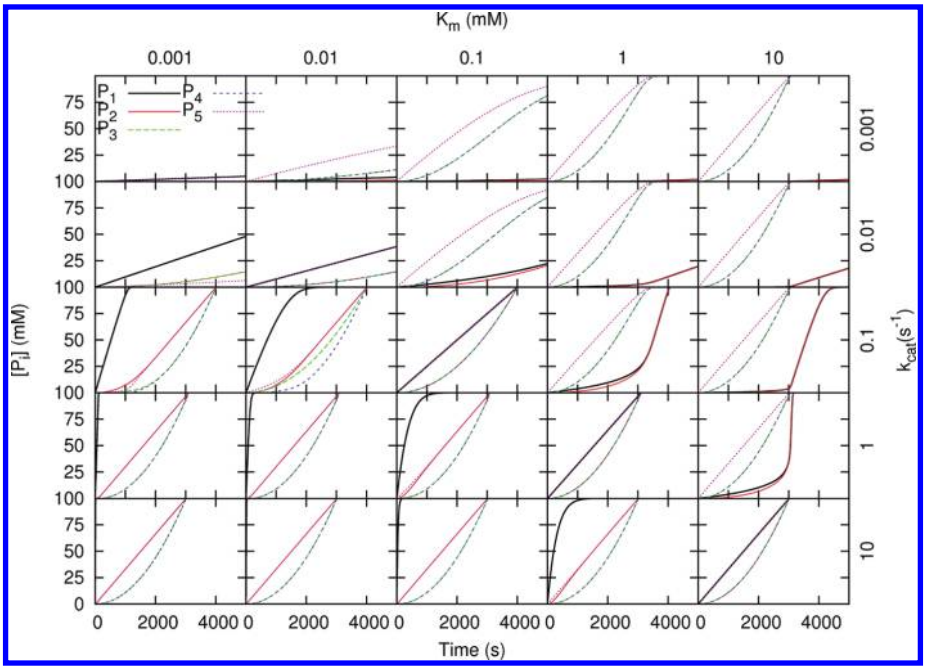

Figure 4. Reaction kinetics profiles for monomer liberation from a pentamer for a matrix of k_{cat} and K_M variation at the S_1 cleavage site. Kinetic parameters for other cleavage sites are $k_{cat} = 0.1\ s^{-1}$ and $K_M = 0.1$ mM.

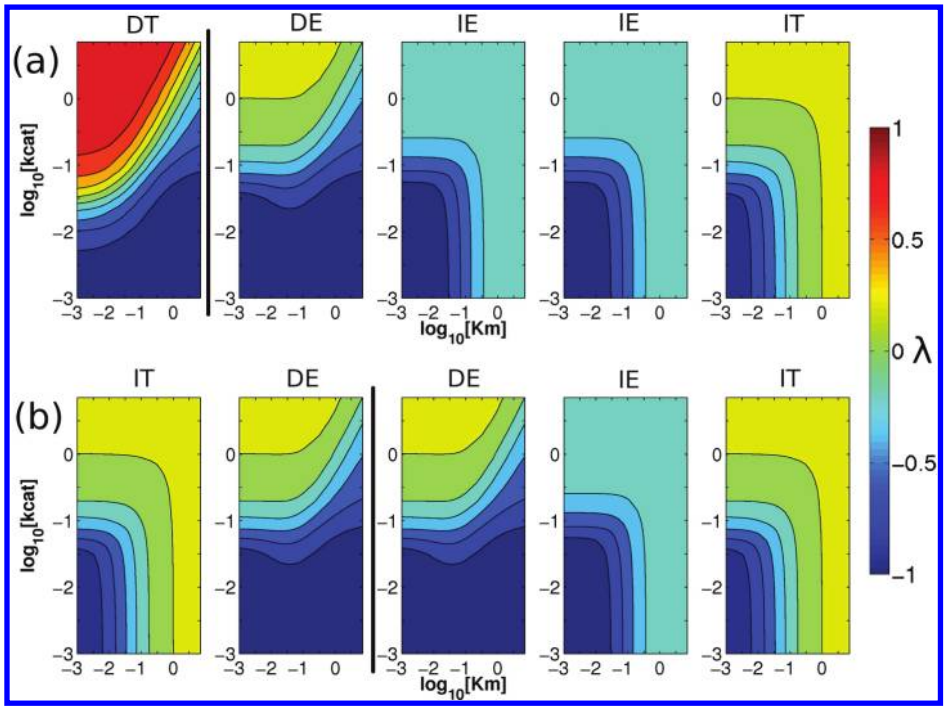

Figure 5. Sensitivity landscape using the normalized integral of concentration of each monomer species, λ (defined in eq 17), up to the characteristic time scale τ_c as a function of varying of kinetic parameters k_{cat} (s^{-1}) and K_M (mM) at the (a) S_1 and (b) S_2 cleavage sites (denoted by black lines). Default kinetic parameters for nonvarying cleavage sites are $k_{cat} = 0.1\ s^{-1}$ and $K_M = 0.1$ mM. Four distinct classes of monomer emerge under parameter variation: directly affected terminal monomers (DT), directly affected embedded monomers (DE), indirectly affected embedded monomers (IE), and indirectly affected terminal monomers (IT).

practically instantaneously and therefore P_2 behaves as though it were a terminal monomer in a heterotetramer.

By contrast, the indirect effects of parameter variation exhibit different behavior; increase in both k_{cat} and K_M results in an increase in the liberation rate of both P_3, P_4, and P_5, and there is a clear turning point in the isocontours of liberation. The indirect effect of parameter alteration is therefore complementary when increasing both parameters. Furthermore, sensitivity is dependent on the region in the parameter landscape; increasing K_M for a given k_{cat} can have no effect on liberation for over 2 orders of

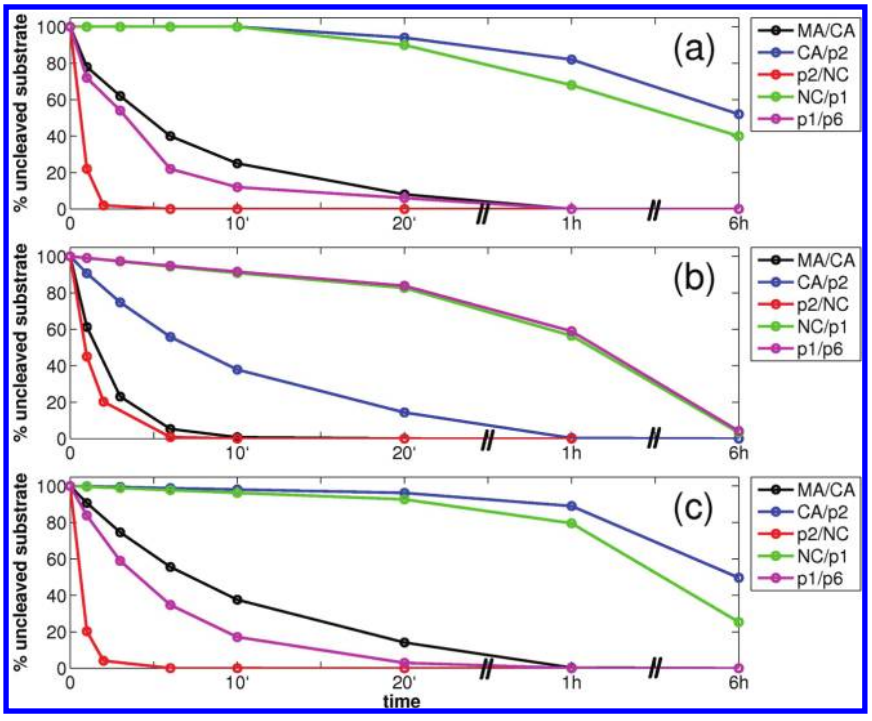

Figure 6. Comparison of the percentage uncleaved substrate for HIV-1 catalayzed Gag polyprotein degradation between (a) experimental data[19] (see Methods), (b) the reaction kinetics model implemented here using the closest set (set 1) of experimentally derived kinetic parameters by Tözsér et al.[22] and initial conditions $[E_t] = 0.18\ \mu M$ and $[S_{gag}](0) = [P_{1,6}](0) = 3.6$ nM from experiment,[19] and (c) the reaction kinetics model with kinetic parameters fitted within 1 order of magnitude difference to set 1.

magnitude followed by a sharp change within 1 order of magnitude. Terminal monomers are liberated faster than embedded ones; thus at high k_{cat}—high K_M, while indirect embedded monomers P_3 and P_4 tend to $\lambda = 0$, corresponding to embedded monomers in a heterotetramer, the indirect terminal monomer P_5 tends to $\lambda = 0.25$, corresponding to a terminal monomer in a heterotetramer.

For S_2 variation, only three of the four classes of monomer are exhibited, there being no directly affected terminal monomer. Direct effects on embedded monomers P_2 and P_3 are identical to each other as well as to those of P_2 when varying S_1. Furthermore, the sensitivity landscape of indirectly affected embedded and terminal monomers are also identical to those obtained when varying S_1; indirect effects act via competition among substrates for the free enzyme.

C. Kinetics of Gag Polyprotein Processing. Reaction kinetics of Gag polyprotein (a heterohexamer, $n = 6$) processing were investigated based on available kinetic parameter data[22] and in vitro Gag cleavage experiments.[19] The initial conditions for enzyme concentration and initial Gag concentration were derived (see Methods) as $[E_t] = 0.18\ \mu M$ and $[S_{gag}](0) = [P_{1,6}](0) = 3.6$ nM. Obtaining the correct parameter set to test against a particular experiment is not trivial. Both the cleavage and parameter determination experiments need to be carried out under the same conditions of pH and temperature. The closest parameter set was that of Tözsér et al.[22] at pH 5.6 and $T = 37\ ^\circ C$ (see set 1 in Table 1, Methods section), while Gag processing experiments were carried out under pH 7.0 and $T = 30\ ^\circ C$. As this range of both temperature and pH heavily affects catalytic activity of HIV-1 protease,[23] quantitative comparison with experiment cannot be expected. Parameter estimation remains a major challenge in complex chemical systems biology, and it is thus not surprising that an exact parameter match is not available. Furthermore, only an estimate of the initial conditions can be made from a set of in vitro assays in which Gag is derived from a Gag-containing rabbit reticulocyte lysate system.[19] Nonetheless, it is instructive to investigate the qualitative similarity of the reaction kinetics for the given kinetic parameter set as well as the degree to which model-fitting can recover the experimental profile.

Figure 6 shows the reaction kinetics in terms of the percentage of uncleaved substrate at each cleavage site junction for (a) the experimental data set,[19] (b) the model prediction using parameter set 1 (see Methods), and (c) the prediction using the optimal parameter set (OPS) determined via model-fitted variation of the kinetic parameters within 1 order of magnitude (see Methods).

In principle, the model describes the reaction kinetics of Gag processing well (see Figure 6). The p2-NC, MA-CA, and NC-p1 cleavage sites are processed with similar decay curves to that obtained in experiment. However, the CA-p2 site decays faster than experiment while the p1-p6 site decays slower than experiment (Figure 6a and b). Comparing all experimentally available values from the similar curve by Pettit et al.[19] with corresponding values from our study yields a correlation coefficient of $\kappa = 0.51$. The poor overall correlation is due to the lack of agreement exhibited by the CA-p2 and p1-p6 curves already mentioned.

A likely possibility for the lack of quantitative agreement is due to the above-mentioned mismatch between the experimental conditions. Other partial or full kinetic data sets show up to 2 orders of magnitude variation for various kinetic parameters (see Table 1); indeed for available cleavage-site parameters, the k_{cat}/K_m ratio is at least 1 order of magnitude greater at pH 5.6, at which the degradation was modeled in our simulations, than for pH 7, at which the in vitro experiment was performed. Therefore,

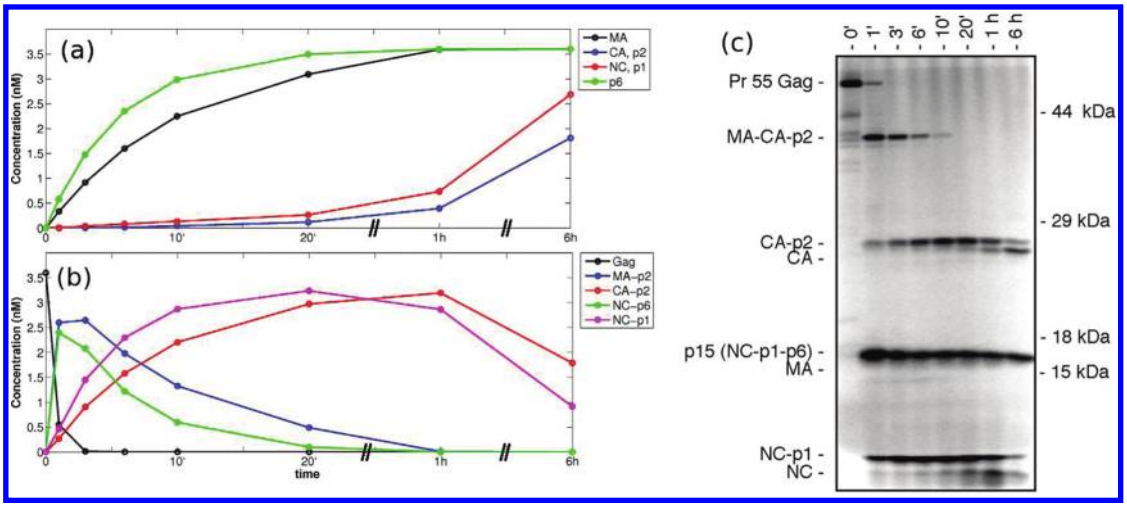

Figure 7. Accounting for complete HIV-1 protease-catalyzed Gag degradation using model-fitted parameters. Time evolution of (a) concentration of final monomeric products (MA, CA, p2, NC, p1, and p6) and (b) concentration of intermediate and initial Gag (MA-p6) species. The kinetic parameter set was the optimal parameter set (OPS) determined from a variation of the Tözsér et al.[22] set within 1 order of magnitude. Initial conditions were $[E_t] = 0.18\ \mu M$ and $[S_{gag}](0) = [P_{1,6}](0) = 3.6$ nM derived from experiment[19] (see Methods). (c) Reprint (with permission) of time evolution of species from experimental result of Pettit et al.[19] for ease of comparison.

in order to determine whether the difference in kinetic parameters entirely accounts for the discrepancy between experiment and model, we performed simulations of Gag processing for multiple variations of each kinetic parameter. Parameter fitting results in an optimal parameter set (OPS) that describes the decay of cleavage sites accurately (Figure 6c). Not only is the correct order of cleavage established for all cleavage sites, but the characteristic time for complete decay is rectified. MA-CA is cleaved completely within 1 h, CA-p2 cleavage slows down substantially (10% cleavage after 1 h), and p1-p6 cleavage accelerates (complete cleavage within 1 h) compared with Figure 6b. The variation required to obtain this match is within 1 order of magnitude for each kinetic parameter, well within the variation exhibited by alternative experimental data sets (see Table 1). The correlation coefficient increases to $\kappa = 0.99$.

Further agreement is noted for the time evolution of emergent monomer species (Figure 7a) as well as transient intermediate products (Figure 7b), using the model-fitted parameters. Of important note is that because these curves were not used in the evaluation of the optimal parameter set (only the match between the percentage cleaved substrates were used), it allows our model to be tested using the model-fitted parameters in a completely predictive way. Unfortunately, these curves are not numerically comparable to corresponding gel-electrophoresis results obtained in the study by Pettit et al.[19] (Figure 1B therein), but nonetheless show a striking resemblance. For ease of comparison, the results obtained by Pettit et al.[19] are reprinted as (Figure 7c).

For emerging monomers (Figure 6a) the concentration of MA corresponds very well to experiment, with a high concentration emerging after just a few minutes. NC emergence corresponds qualitatively to experiment with significant concentration emerging beyond 1 h. CA concentration increases, becoming significant after 6 h in our simulations consistent with experiment. Gag (MA-CA-p2-NC-p1-p6) decay occurs swiftly within several minutes as it does in experiment (Figure 6b). There are strong initial concentration peaks of NC-p1-p6 at around 1 min and MA-CA-p2 at around 3 min followed by a long decay extending over an hour for both these intermediate species. This is matched by the experimental results for MA-CA-p2 which show a clear maximum after 1 min; the proximity of the NC-p1-p6 and MA lines prevents NC-p1-p6 decay from being discerned clearly on the gel. However, the decrease in width of the gel-line after 3 min also indicates decay of the NC-p1-p6 species at that point, consistent with our results. Also the CA-p2 dimer is experimentally observed to peak at around 20 min and then decay completely over several hours. This agrees qualitatively with our results for which the peak occurs at 40 min followed by a long decay over several hours. Finally, NC-p1 peaks at 20 min and then exhibits a long slow decay too, although faster than the CA-p2 dimer, as noticeable in the experimental results.

IV. DISCUSSION

Summarizing our results, numerical implementation of the kinetic model for competitive heteropolymeric cleavage shows that differential liberation of various final products emerges naturally from the structure of the equations. The increased rate of terminal monomer release as compared to that of embedded monomers arises as the latter requires double the number of cleavage processes. Furthermore, the intrinsic coupling between the rates of liberation of all monomers is demonstrated; that is, changing the kinetic parameters of one cleavage site to alter the liberation rate of connected monomers can alter the rate of liberation of all other monomers too.

Our results demonstrate the counteracting effects of increasing both k_{cat} and K_M for monomers connected to the corresponding cleavage site. Interestingly, the indirect effect on the nonconnected monomers is more subtle. A higher k_{cat} at one cleavage site increases the production rate of both nonconnected and connected monomers. Conversely, decreasing K_M at a cleavage site, while increasing the production rate of connected monomers, decreases it for nonconnected monomers.

The kinetics of monomers not directly connected to the varied cleavage site is, in most extreme regimes of k_{cat} and K_M,

Table 1. Kinetic Parameters for Gag Polyprotein Processing by HIV-1 Protease

		S_1	S_2	S_3	S_4	S_5
cleavage site		MA-CA	CA-p2	p2-NC	NC-p1	p1-p6
set 1[c22]	K_M	0.15	0.01	0.05	0.17[a]	1.2[a]
(pH 5.6, T = 37 °C)	k_{cat}	6.8	0.09	3.7	0.15[a]	0.98[a]
set 2[31]	K_M	3.75	0.37	3.0	–	>5.0
(pH 5.5, T = 25 °C)	k_{cat}	23.0	2.6	41.0	–	<0.25
set 3[32]	K_M	1.5	–	0.5	–	6.4
(pH 5.0, T = 37 °C)	k_{cat}	51.8	–	58.8	–	12.7
set 4[20]	K_M	5.3	0.11	–	–	–
(pH 5.0, T = 37 °C)	k_{cat}	20.0	2.0	–	–	–
set 5[20]	K_M	87.0[b]	3.14	–	–	–
(pH 7.0, T = 37 °C)	k_{cat}	114.0	2.2	–	–	–
fitted OPS[d]	K_M	0.15(1)	0.05(5)	0.025(0.5)	0.85(0.5)	0.12(0.1)
	k_{cat}	1.36(0.2)	0.009(0.1)	3.7(1)	0.03(0.2)	1.96(2)

[a] From Feher et al.[33] [b] Limited substrate concentration, K_M in mM, k_{cat} in s^{-1}. [c] This set alone was used in the reaction kinetics simulations. [d] Optimal parameter set. Factor change relative to set 1 in parentheses.

insensitive to the alteration of terminal cleavage site processing except in the low k_{cat}, low K_M regime in which there is effective inhibition of all processing. However, there is a sensitive regime within 1 order of magnitude of difference to other cleavage sites where the subtle interplay of competing effects of k_{cat} and K_M causes critical modulation of the emergent products.

Furthermore, as alteration of k_{cat} and K_M can exert competing forces on the reaction kinetics, it is possible to obtain similar kinetics from different kinetic parameter sets. For a more complex scenario in which multiple heterogeneities exist in the kinetic parameters across the original heteropolymer, many combinations of k_{cat} and K_M could give the same kinetics. It is thus difficult to classify the reaction kinetics as being due to any given kinetic parameter set. Instead, the kinetics emerges from the structure of the equations which encode the coupled nature of the processing at each cleavage site.

Application of the numerical scheme to the Gag polyprotein cleavage by HIV-1 protease in vitro reveals notable similarity with experiment, given that the conditions in which the kinetic parameter set has been determined varies from the conditions in which the Gag decay is measured. Sensitivity analysis demonstrates that variation of the kinetic parameters within the 2 orders of magnitude possible in experimental determination is able to provide a good correlation between theory and experiment. This suggests that, provided corresponding model parameters are accurately estimated with respect to the given decay experiments, the scheme developed here can be refined in order to predict medically important quantities such as viral maturation rate[24] and time to attaining infectivity.[25]

Overall, our model captures the process of in vitro HIV-1 protease-catalyzed Gag degradation with striking accuracy. First, using the closest available parameter set allows qualitative similarity for a number of cleavage sites, despite the difference in pH and temperature conditions. As the reaction kinetics of a heteropolymer is sensitive within the pH range of variation described (see Figure 5), it is entirely plausible that kinetic parameters for the corresponding experimental conditions would allow accurate quantitative comparison. However, it raises the question of whether a Michelis−Menten type reaction kinetics model alone is sufficient for explaining the process. Variation of the kinetic parameters within 1 order of magnitude of the closest experimental parameter set allows a good fit with experiment, confirming the appropriateness of the reaction kinetics model. This is confirmed by the correlation of the time evolution of intermediate and final species, even though their time evolution is not used to determine the optimal parameter set. An alternative consideration is that mismatch between the model and experiment may be explained by conformational shielding effects for specific cleavage sites. For example, CA-p2 and NC-p1 cleavage is largely insignificant until other cleavage processes are near completion. However, such phenomena need not require shielding effects in order to arise. Rather, our results state that Gag decay is a continuous process; the order of emergence of the various structural proteins that form a HIV virion, at least in vitro, can be determined from subtle changes in the kinetic parameters and do not require more complicated models.

The intrinsic coupling exhibited in our model has important consequences for the interpretation of the processing rates of complex biochemical reactions. In Gag cleavage by HIV-1 protease, in particular, much emphasis has been placed on the specificity ratio k_{cat}/K_M of single rate limiting reactions as being the sole determinant of reaction kinetics.[26,27] The scheme developed here shows that it is necessary to consider the intrinsically coupled effect of altering the specifics of *all* processes involved in the complex set of reactions. Our approach provides a more robust and global description of the catalytic efficiency of the complex process.

For example, capsid (CA) liberation is critical for the formation of the conical capsid shell of HIV-1 protease.[28] It is thus a good first approximation to consider that CA-p2 cleavage and/or MA-CA cleavage affect the liberation rate of CA. Regulation of this process and thus the maturation of HIV virions has been attributed to pleiotropic effects[20] where the inhibition of the p2-NC cleavage site has up-regulated production of CA (which is unconnected to the cleavage site). We show that such regulation is governed by the structure of the equations describing the coupled reaction kinetics of Gag degradation; that is, altering one cleavage site rate also has a marginal indirect effect on non-connected monomers. Furthermore, it is likely that compensatory resistance mutations,[29] that act by enhancing catalytic efficiency of CA production, take advantage of the sensitivity

exhibited by monomer production rates in the critical modulation regime described in our model. Such mutations need not reside at the CA-p2 site; indeed they are also found in pleiotropic regions such as the NC-p1 and p1-p6 sites.[30] Our model thus describes a more meaningful description of the overall catalytic efficiency of the protease and, indeed, any enzyme in the competitive heteropolymeric cleavage class.

Although our model supports thermodynamic stochastic collision for in vitro Gag processing, it is likely that its in vivo kinetics differ significantly due to the constraining geometry of the virion, in which immature Gag is assembled in a hexameric lattice with only 8 nm spacing.[28] This coupled to the fact that in vivo Gag exists together with a smaller relative population of GagPol, from which the protease must autoprocess itself and form homodimers to acquire functional enzyme form, suggests that more accurate monitoring of in vivo maturation requires a more complex, though still tractable, kinetic model. Whether this would change the underlying kinetics that emerges from a Michelis−Menten type scheme remains to be seen. Interestingly, if more complicated phenomena direct in vivo processing, then from the perspective of a reaction kinetics model, this would be naturally exhibited in the form of kinetic parameters for cleavage sites that were dependent on the intermediate species in which they existed. Finally, the model developed here provides a theoretical baseline to evaluate the degree to which a heteropolymeric degradation process can be described in terms of free diffusion and thermodynamically driven stochastic collision; it also provides an enhanced measure of catalytic efficiency and viral maturation rate than current approaches predicated solely on single k_{cat}/K_M ratios.

V. CONCLUSION

The reaction kinetics scheme developed here provides a theoretical description of the rate of formation of any intermediates arising within a heteropolymeric cleavage reaction as well as the rate of formation of the final products. Such a development forms the basis for predictive kinetic models of any chemical or biochemical process that proceeds under such a mechanism. In particular, the in vitro rate of production of mature proteins from long polyprotein chains cleaved by viral proteases is now predictable. Future investigations that determine the required enzymatic parameters to populate such a scheme will allow this model to be elaborated in order to track and predict the time for viral maturation and infectivity.

VI. METHODS

Equations 13−14 were numerically integrated on a computer using a time step of dt = 1 s and a fourth-order Runge−Kutta scheme. The algorithm was implemented as follows: (a) Define initial conditions (t = 0): polymericity number (n), concentration of $[P_{i,k}]$, total enzyme concentration $[E_t]$, (b) define kinetic parameters for each cleavage site (K_M and k_{cat}), (c) calculate Z_M and finite difference in concentration of each species (d$[P_{i,k}]$) for each step within the fourth-order Runge−Kutta scheme and integrate to obtain new concentrations at $[P_{i,k}](t + dt)$, and (d) advance time step and return to step (c).

Kinetic parameter sets for Gag polyprotein processing by HIV-1 protease were taken from Tözsér et al.[22] and are provided together with a comparison with other sources in Table 1. Gag is a linear heterohexamer (n = 6) composed of MA, CA, p2, NC, p1, and p6 proteins (MA-CA-p2-NC-p1-p6). Reaction kinetics of Gag was modeled with initial conditions of $[E_t]$ = 0.18 μM, $[P_{1,6}](0)$ = 3.6 nM and derived from estimates of the corresponding experimental quantities.[19] $[E_t]$ was based on 0.2 μg of purified recombinant HIV-1 protease in 50 μL aliquots. Determination of initial concentration of Gag ($[S_{gag}](0) = [P_{1,6}](0)$) in molar quantities is less trivial and requires estimation from a Gag-containing rabbit reticulocyte system. Based on the typical protein yield 50−200 ng per 50 μL reaction mixture (when using 2 μg RNA; as given in the protocol of the manufacturer Promega), the use of 1 μg RNA and the 10-fold dilution, we estimate a Gag mass of 10 ng/50 μL aliquot resulting in a concentration of $[S_{gag}](0) = [P_{1,6}](0)$ = 3.6 nM. The kinetics were compared to Gag decomposition experiments performed at pH 7.0 and T = 30 °C.[19]

Simulations were also performed for a range of variation of the kinetic parameters. Both k_{cat} and K_m for each cleavage site were varied between a factor of 0.1 and 10 (specifically, 0.1, 0.2, 0.5, 2, 5, and 10) of set 1. The factor most closely matching the time evolution of the individual cleavage site decay was used as an estimate of the best fit parameters for the corresponding cleavage site in the overall best fit set. This collection of independently optimized parameters was then used as the optimal parameter set (OPS) for the fitted model (Table 1). The time evolution of full Gag degradation was then charted using the OPS. Again, the same initial conditions were used as experiments.

VII. APPENDIX

Here we derive the expression for the rate of liberation of a terminal monomer, P_1, under the conditions of equivalent kinetic parameters along all cleavage sites of a heteropolymer of length n and an excess of concentration of substrate. The rate of liberation of a terminal monomer P_1 is equivalent to the rate of cleavage of the S_1 cleavage site. We thus have from eq 2

$$\nu_1 = \nu^1 = \frac{k^1_{cat} \cdot [S_1] \cdot [E_t]}{K^1_M(1 + \sum_{j=1}^{n-1} [S_j]/K^j_M)} \tag{18}$$

which can be written as

$$\nu_1 = \frac{k^1_{cat} \cdot [E_t]}{K^1_M} \cdot \frac{1}{(1/[S_1] + \sum_{j=1}^{n-1} [S_j]/K^j_M[S_1])} \tag{19}$$

However, for equivalent kinetic parameters ($K^1_M = K^2_M ... = K^{n-1}_m$ and $k^1_{cat} = k^2_{cat} ... = k^{n-1}_{cat}$) the time evolution of all cleavage site concentrations $[S_r]$ must be equal ($[S_1](t) = [S_2](t) ... = [S_{n-1}](t)$), so the above equation simplifies to

$$\nu_1 = \frac{k^1_{cat} \cdot [E_t]}{K^1_M} \cdot \frac{1}{(1/[S_1] + (n-1)/K^1_M)} \tag{20}$$

and under the condition that $[S_1] \gg K^1_M$, the contribution of $1/[S_1]$ in the denominator is negligible and we can approximate further to

$$\nu_1 \approx \frac{k^1_{cat} \cdot [E_t]}{n-1} = \text{constant} \tag{21}$$

as described by eq 15.

AUTHOR INFORMATION

Corresponding Author
*E-mail: kashif.sadiq@upf.edu, syedkashifsadiq@gmail.com.

ACKNOWLEDGMENT

This research has been partially supported by the EU-funded ViroLab project (IST-027446). S.K.S. acknowledges support from a European Commission FP7Marie Curie Intra-European Fellowship. V.M. acknowledges support from the Hungarian Scientific Research Fund (OTKA NF72791) and a Bolyai János Research Fellowship of the Hungarian Academy of Sciences.

REFERENCES

(1) Turing, A. M. *Philos. Trans. R. Soc. London, Ser. B* **1952**, *237*, 37–72.
(2) Kitano, H. *Science* **2002**, *295*, 1662–1664.
(3) Tyson, J. J.; Chen, K.; Novak, B. *Nat. Rev. Mol. Cell Biol.* **2001**, *2*, 908–916.
(4) Aldridge, B. B.; Burke, J. M.; Lauffenburger, D. A.; Sorger, P. K. *Nat. Cell Biol.* **2006**, *8*, 1195–1203.
(5) Heinrich, R.; Rapoport, S. M.; Rapoport, T. A. *Prog. Biophys. Mol. Biol.* **1977**, *32*, 1–82.
(6) Tyson, J. J. *Proc. Natl. Acad. Sci. U.S.A.* **1991**, *88*, 7328–7332.
(7) Wattis, J. A. D.; Coveney, P. V. *J. Phys. Chem. B* **1999**, *103*, 4231–4250.
(8) Cornish-Bowden, A. *Fundamentals of Enzyme Kinetics*; Portland Press: London, U.K., 2004.
(9) Briggs, G. E.; Haldane, J. B. S. *Biochem. J.* **1925**, *19*, 338–339.
(10) Schauer, M.; Heinrich, R. *Math. Biosci.* **1983**, *65*, 155–170.
(11) Segel, L. A. *B. Math. Biol.* **1988**, *50*, 579–593.
(12) Wattis, J. A. D.; Coveney, P. V. *J. Phys. Chem. B* **2007**, *111*, 9546–9562.
(13) Hanson, K. R. *Biochemistry* **1962**, *1*, 723–734.
(14) Hiromi, K.; Ono, S. *J. Biochem.* **1967**, *61*, 654–656.
(15) Leung, Y.; Wong, L. K.; Santer, R.; Alliet, P.; Lee, P. *Comput. Biomed. Res.* **1991**, *24*, 209–221.
(16) Thoma, J. A. *Biochemistry* **1966**, *5*, 1365–1374.
(17) Razzell, W. E.; Khorana, H. G. *J. Biol. Chem.* **1959**, *234*, 2105–2113.
(18) Wlodawer, A.; Miller, M.; Jaskólski, M.; Sathyanarayana, B. K.; Baldwin, E.; Weber, I. T.; Selk, L. M.; Clawson, L.; Schneider, J.; Kent, S. B. H. *Science* **1989**, *245*, 616–621.
(19) Pettit, S. C.; Henderson, G. J.; Schiffer, C. A.; Swanstrom, R. *J. Virol.* **2002**, *76*, 10226–10233.
(20) Pettit, S. C.; Moody, M. D.; Wehbie, R. S.; Kaplan, A. H.; Nantermet, P. V.; Klein, C. A.; Swanstrom, R. *J. Virol.* **1994**, *68*, 8017–8027.
(21) Rodriguez-Fernandez, M.; Mendes, P.; Banga, J. R. *Biosystems* **2006**, *83*, 248–265.
(22) Tözsér, J.; Bláha, I.; Copeland, T. D.; Wondrak, E. M.; Oroszlan, S. *FEBS Lett.* **1991**, *281*, 77–80.
(23) Hyland, L. J.; Tomaszek, T. A., Jr.; Roberts, G. D.; Carr, S. A.; Magaard, V. W.; Bryan, H. L.; Fakhoury, S. A.; Moore, M. L.; Minnich, M. D.; Culp, J. S.; et al. *Biochemistry* **1991**, *30*, 8441–8453.
(24) Ivanchenko, S.; Godinez, W. J.; Lampe, M.; Kräusslich, H. G.; Eils, R.; Rohr, K.; Bräuchle, C.; Müller, B.; Lamb, D. C.; Mothes, W. *PLoS Pathog.* **2009**, *5*, e1000652.
(25) Perelson, A. S.; Neumann, A. U.; Markowitz, M.; Leonard, J. M.; Ho, D. D. *Science* **1996**, *271*, 1582–1586.
(26) Gulnik, S. V.; Suvorov, L. I.; Liu, B.; Yu, B.; Anderson, B.; Mitsuya, H.; Erickson, J. W. *Biochemistry* **1995**, *34*, 9282–9287.
(27) Ohtaka, H.; Schon, A.; Freire, E. *Biochemistry* **2003**, *42*, 13659–13666.
(28) Briggs, J. A. G.; Simon, M. N.; Gross, I.; Kräusslich, H. G.; Fuller, S. D.; Vogt, V. M.; Johnson, M. C. *Nat. Struct. Mol. Biol.* **2004**, *11*, 672–675.
(29) Nijhuis, M.; Schuurman, R.; de Jong, D.; Erickson, J.; Gustchina, E.; Albert, J.; Schipper, P.; Gulnik, S.; Boucher, C. A. B. *AIDS* **1999**, *13*, 2349–2359.
(30) Bally, F.; Martinez, R.; Peters, S.; Sudre, P.; Telenti, A. *AIDS Res. Hum. Retroviruses* **2000**, *16*, 1209–1213.
(31) Maschera, B.; Darby, G.; Palu, G.; Wright, L. L.; Tisdale, M.; Myers, R.; Blair, E. D.; Furfine, E. S. *J. Biol. Chem.* **1996**, *271*, 33231–33235.
(32) Ermolieff, J.; Lin, X.; Tang, J. *Biochemistry* **1997**, *36*, 12364–12370.
(33) Feher, A.; Weber, I. T.; Bagossi, P.; Boross, P.; Mahalingham, B.; Louis, J. M.; Copeland, T. D.; Torshin, I. Y.; Harrison, R. W.; Tözsér, J. *Eur. J. Biochem.* **2002**, *269*, 4114–4120.